

An Image Restoration Technique for the Removal of Cosmic-Ray Hits from Dithered Images

WOLFRAM FREUDLING

Space Telescope–European Coordinating Facility, European Southern Observatory, Karl-Schwarzschild-Strasse 2,
 85748 Garching bei München, Germany
 Electronic mail: wfreudli@eso.org

Received 1994 June 6; accepted 1994 October 24

ABSTRACT. A method is proposed to find and remove cosmic rays from stacks of images which are *not* registered. Such dithered images obtained with undersampling cameras, such as the Wide Field and Planetary Camera 2 (WFPC2) on board the *Hubble Space Telescope*, can be used to recover some of the resolution lost by a large pixel size. The proposed method simultaneously cleans the images of cosmic rays and deconvolves them. Cosmic-ray hits are dynamically identified at each iteration. The output is a combined and restored image and a list of cosmic-ray hits for each of the input images. The final lists of cosmic-ray hits are useful even if a restoration of the images is not desired. A simulated application of the method to WFPC2 images is presented.

1. INTRODUCTION

The Wide Field and Planetary Camera 2 (WFPC2), is the primary instrument of the *Hubble Space Telescope* (*HST*). Compared to most ground-based CCD systems, this camera is limited by two additional factors. Inevitably, because of being stationed in space, the number of cosmic-ray hits (CR hits) per time and area is much larger than the numbers familiar from cameras on the ground. The second factor is a technical limitation, and is the fact that the size of the CCD pixels is such that the point-spread function (PSF) is significantly undersampled. This is true even for the high-resolution CCD in the camera, the PC; and undersampling is severe for the wide-field CCDs. Because of the much improved PSF, this undersampling is more severe for the aberration corrected WFPC2, which was installed as a replacement of the previous Wide Field and Planetary Camera (WF/PC) in December 1993.

Images can be corrected for both of these limitations if suitable observing strategies are employed. Unfortunately, the simplest strategies designed to simplify later correction for the two effects are mutually exclusive. On the one hand, in order to ease the removal of CR hits from images, the total integration time is usually split into a number of exposures which are *registered*, so that the flux in different exposures can be compared on a pixel by pixel basis. Such CR splits are standard *HST* observing procedure, and this approach to identify CR hits on WF/PC images has been discussed in detail by Windhorst et al. (1994). On the other hand, it has been suggested to recover some of the resolution lost through undersampling by dithering the exposures on a subpixel level, i.e., shift the camera by an amount less than the size of the pixels between exposures. One approach to combine such dithered images was suggested by Lucy (1991) and implemented by Hook and Lucy (1992, 1993). In their treatment, some of the resolution lost through undersampling is recovered by simultaneously deconvolving several dithered images. However, the effect of CR hits on deconvolution can be devastating (e.g., King et al. 1991; Windhorst et al. 1994 and references therein), and the sub-pixel shifts between the ex-

posures prevents the application of simple filtering techniques to identify and remove CR hits.

CR removal programs acting on single images are in common use for ground-based CCD work and are available in most image processing packages. Usually, CR hits are removed by interpolation of flux from pixels adjacent to the CRs. Such a procedure could be applied to the individual images before co-adding them. However, it is difficult to identify CR hits on severely undersampled images. In addition, the application of such a procedure would defeat the purpose of taking dithered images for later resolution enhancement, because the interpolation locally decreases the resolution.

The purpose of this paper is to suggest and demonstrate a method to identify and remove CR hits from images of the same field which are *not* registered by simultaneously applying the resolution enhancement technique by Hook and Lucy and dynamically masking CR hits in each iteration. The method does not use any interpolation, and uses the full information content of the observed images. The method can be used either by directly using the restored, co-added and CR cleaned image as the final result, or by using the list of CR hits for further processing of the images without actually utilizing the restoration.

The details of the suggested method are given in Sec. 2, and a simulated application is presented in Sec. 3. The conclusion of this experiment for the strategy an observer should deploy are given in the final Sec. 4.

2. CO-ADDITION AND CR REMOVAL

2.1 Method

Hook and Lucy (1992) have described a method for co-adding images with different PSFs, which is a straightforward generalization of the Richardson-Lucy image restoration method (Richardson 1972; Lucy 1974). In their iterative scheme, a multiplicative correction factor $t(x,y)$ to the current estimate for the image $o^k(x,y)$ is computed in iteration k as

$$t(x,y) = \sum_n w_n t_n(x,y) \star \text{psf}_n(x,y), \quad (1)$$

$$t_n(x,y) = \frac{i_n(x,y)}{i_n^k(x,y)}, \quad (2)$$

where n labels the input images $i_n(x,y)$, $i_n^k(x,y)$ is the current estimate of the image $o_k(x,y)$ convolved with the PSF for image $i_n(x,y)$, w_n is the weight of the input image, and \star indicates a correlation. One suggested application of this procedure is to add images of the same fields which are shifted relative to each other by a fraction of the pixel size, which corresponds to a relative shift of the PSFs.

This co-addition scheme can be modified to include a CR treatment. Once the estimate $o_k(x,y)$ is a good representation of the observed images, CR hits can be easily identified on the correction factor t_n before the convolution and Eq. (1) can be modified to

$$t_n(x,y) = \begin{cases} 0 & \text{if CR hit} \\ i_n(x,y) / i_n^k(x,y) & \text{else} \end{cases} \quad (3)$$

The effect will be that there are “holes” in the final correction factor image, which are of the shape of negative PSFs for single pixel events. Those holes can overlap due to close CR hits either on the same image or on different images. The holes in the correction factor from each image $h_n(x,y)$ can be easily modeled by creating masks at the CR removal stage which are unity everywhere but at the position of the CR hit, where they are zero. Such masking of bad pixels within the Richardson-Lucy iteration is a special case of a flat-field correction (Snyder et al. 1993; see also White 1994) and is implemented in Hook and Lucy’s code. The difference here is that the masks are dynamically created, i.e., evolve from iteration to iteration. From those masks, the holes are computed

$$h_n(x,y) = w_n \text{mask}_n \circ \text{psf}_n(x,y), \quad (4)$$

where \circ indicates a convolution.

Those holes can be filled by locally increasing the weight of the images not affected by the CR hit. If the PSF is well sampled, not all information about the affected pixels is lost because the information contents in adjacent pixels is not independent. This information can also contribute to fill the flux holes. In general, Eq. (2) can be changed to

$$t(x,y) = \sum_n w_n(x,y) [t_n(x,y) \star \text{psf}_n(x,y)], \quad (5)$$

where the weights $w_n(x,y)$ now depend on the position in the image and are computed from

$$w_n(x,y) = w_n + \frac{h_n(x,y)}{\sum_m h_m(x,y)} \sum_m [w_m - h_m(x,y)]. \quad (6)$$

In the special case that there are no CR events on any input image, $h_m(x,y)$ equals w_m everywhere and the method reduces to the original co-addition scheme.

The only problem left is the identification of the CR hits so that Eq. (3) can be applied. The correct identification in

the first iteration is very critical because error made then might not be corrected later. For example, if a CR hit is not properly identified in the first iteration, the corrected estimate of the image $o^2(x,y)$ will have a peak at that position, which will make CR detection even less likely in the next iteration. If, on the other hand, a star is wrongly identified as a CR hit in several images, the estimate of the image will become flat at that position and again make it even more likely for the star to be identified as a CR in further iterations. It is therefore important that a good model of the deconvolved image is available before a first attempt is made to identify CR hits.

One way to obtain such a good initial estimate is not to locate the CR hits in the first few iteration, but instead replace the sum in Eq. (2) by the median of the correction factors. This way the CR hits have little impact on the estimate o^k of the image. Such an estimate will of course take poor advantage of all the information in the images. However, after a sufficient number of iterations, the restored image is a good enough model to the data and all correction factors are close to unity. Therefore, at this stage it is easy to identify CR hits on each of the images, e.g., through clipping of pixels which deviate more than the locally expected noise from the estimated observation i_n^k . At this stage, the full CR treatment as described above can start. If only two images of the same object are available, taking the minimum instead of the median of the correction factors should be enough to produce an intermediate model good enough for the CR detection, if the CR hits only produce flux enhancement and if the PSFs are of similar shape.

The detection of CRs at this stage uses the best available estimate of the imaged field and therefore of each of the observed images. It is therefore significantly easier than any direct comparison of the dithered images. Therefore, the proposed algorithm can be used to find CR hits on stacks of dithered images even if a restoration of the images is not desired. The advantage over most other CR finding procedures is that the noise properties and PSF of the observation as well as an estimate of the imaged field are exploited to distinguish between real objects and CR hits.

2.2 Implementation

Hook and Lucy (1992) presented a FORTRAN code which implements their co-adding scheme. This code can be compiled both under IRAF and MIDAS through a special common interface. The relative minor additions to implement the iterative CR scheme were made to this code. Subroutines to determine the median were adopted from the Numerical Recipes (Press et al. 1986).

The CR hit identification was implemented by modeling the noise as a function of flux f as

$$\sigma = \sqrt{\text{ron}^2 + g \cdot f / g}, \quad (7)$$

where the “read-out noise” ron and gain g are user supplied parameters. In general, ron will include all sources of flux independent noise such as the contribution by any background or dark current subtracted before co-adding the images. The expected noise at each pixel is computed from the current model of the observations $i_n^k(x,y)$. All pixels at

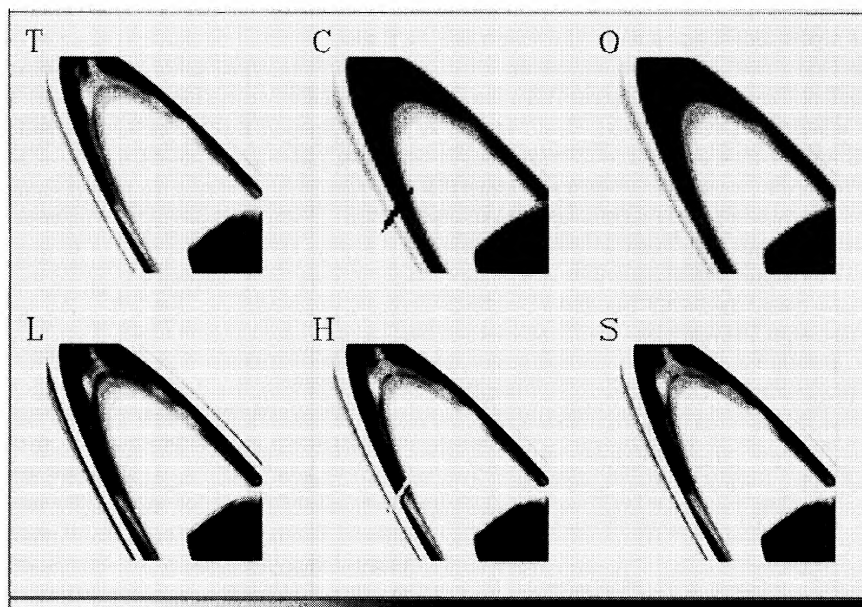


FIG. 1—Simulation of cosmic-ray removal. Image T shows the “true image.” Images C and O are two (out of three) WFPC2 observations of the field. Image C includes two big CR hits, and the grayscale is chosen to show them with high contrast. Image O is shifted relative to image C by $2/3$ of a WFPC2 pixel in x direction. The contrast in image O is lower than in image T. If they were shown with the same grayscale, the outer ring would not be visible. Image L is a Lucy-Richardson restoration of observations of the field not shifted relative to each other. Image H is a co-addition of images C after removal of the CR hits, image O and a similar image not shown. Image S is a co-addition of the same images but with the CR treatment as discussed in the text. Only a section of 200×200 pixels is shown for all images, the simulation was carried out with images of the size 1024×1024 .

which the actual observations deviate from their corresponding model by more than a user-supplied threshold in terms of the expected noise are considered as CR hits. In addition, a radius around each identified CR hit can be specified which is considered to be part of the CR hit.

The program was compiled and tested in IRAF. There are five parameters in the above procedure (in addition to the regular co-adding procedure). They are the number of iterations carried out while using the median (or minimum) instead of the sum of the correction factors, the threshold for the CR identification, the two parameters for the noise model and the optional radius of CR hits.

The memory requirement for the co-addition of N images with this implementation of the CR procedure, which avoids any unnecessary recomputations, is storage for $2N+3$ images in addition to the $3N+5$ images needed for the basic co-addition procedure (without acceleration). All images are stored as double precision numbers.

3. TEST ON SIMULATED WFPC2 OBSERVATIONS

A preliminary version of this idea has been tested both on simulated images and on images taken with the original WF/PC (Freudling 1994a), the camera on board of *HST* which by now has been replaced. Because of the large fraction of light in the wings of the PSF caused by the spherical aberration of the primary mirror, those demonstrations were neither demanding for the identification of CR hits nor for their removal. The purpose of the test on simulated WFPC2 images presented here is to investigate whether such an algorithm works even for the more challenging case of a sig-

nificantly undersampled PSF, which is the case where the largest increase in resolution can be expected from sub-pixel shifts between exposures.

To test the IRAF implementation of the program, a Voyager image of Saturn was used to simulate dithered WFPC2 observations. The original image with 600×900 pixels is a processed image of the whole planet which is in the public domain and has been widely distributed. The image was copied into a bigger 1024×1024 image which matches the background of the original image in order to avoid aliasing effects when the whole image is convolved with the PSF. This image served as the “true” object to be observed, and a part of it is shown in panel T of Fig. 1. A WFPC2 PSF for the center of chip 2 and filter *F555W* of the same size 1024×1024 was created with the simulation software TINYTIM. The PSF was oversampled by a factor of 3, i.e., 3×3 pixels of the PSF image correspond to one WFPC2 pixel. This defines the scale of the “true” image compared to WFPC2 pixels, which resulted in a diameter of the planet of roughly 15 arcsecs, i.e., the size of the planet relative to the pixel size is a roughly realistic presentation of the apparent size of the planet. Three “observed” images were created by convolving the “true” image with three versions of the PSF and subsequently binning every block of 3×3 pixels to create one WFPC2 pixel. The three versions of the PSF function were first the original PSF function, the original shifted by two original pixels along the x axis, and the original PSF shifted by 1 pixel along the x axis and one along the y axis. These shifts correspond to shifts by $2/3$ of a WFPC2 pixel along the x axis, respective $1/3$ of a WFPC2 pixel along the

x and y axes. For real observations with WFPC2, a shift by an integer number of pixels should be added to the subpixel shifts in order to prevent “hot” pixels from covering the same part of the imaged object in different images (Freudling 1994b). One of the images is shown in panel O of Fig. 1. Because of the environment in space, WFPC2 cosmic-ray hits are frequently multipixel events which are much larger than typical cosmic-ray events on images taken with ground-based cameras. Such large events pose a particular challenge to cosmic-ray removal software. Simulations with randomly distributed CR hits have been shown by Freudling (1993). Here, one of the images were degraded by adding two very large cosmic-ray hits at positions on the images where they cover significant small-scale structure. This image is shown in panel C of Fig. 1. These are true cosmic-ray hits as they actually occurred (among many others) within a 100 s exposure with WFPC2 (Freudling 1994c). They have been isolated from the image and placed at the selected positions on the “observed” Saturn image.

The three “observed” images were subsequently processed in three different ways. First, the median was taken of three versions of the *unshifted* “observed” image to remove the cosmic rays in the case that observations were taken without shifts between images. The resulting image is indistinguishable from panel O in Fig. 1, i.e., no traces of the CR hit was left. Each pixel in the image was then subdivided in 3×3 pixels of the same flux. Subsequently, the image was deconvolved with 100 iterations of a revised Lucy-Richardson restoration, which takes into account the fact that the PSF is sampled on a finer grid than the image (Lucy and Baade 1989). This is an attempt to extract the maximum amount of spatial resolution from a single image. The resulting restored image is shown in panel L in Fig. 1. The gray-scale of the figure was chosen to show the details of the outer faint ring. The image shows some structure on scales smaller than the original pixel size. However, there are also some artifacts roughly of the original pixel size, which reflects the fact that the Lucy-Richardson restoration recovers only part of the information lost through undersampling of the PSF by the simulated observation.

Next, the three “observations” shifted relative to each other were processed in the following way. The CR hits were replaced by the average flux on the true image at the position of the CR hits. This is what a good CR-cleaning algorithm might achieve on a single image. A median of the images is not an option here because the images are shifted relative to each other. The CR-cleaned shifted images were then co-added with the program by Hook and Lucy (1992). The resulting image is shown in panel H of Fig. 1. Note the much finer detail in the outer rings on scales smaller than the WFPC2 pixels, in particular the fluctuations along the ring which have been lost in any single observations (panel O) and cannot be recovered from the aligned images (panel L). However, at the position of both CR hits, the resulting co-added image is significantly degraded and deviates stronger from the “true” image (panel T) than the unshifted, restored image (panel L). Therefore, the observing strategy of sub-pixel shifts resulted in enhanced resolution in most parts of

the final image, but degraded resolution at the position of the CR hits.

Finally, the three shifted images were simultaneously restored and CR cleaned as described in Sec. 2. Because WFPC2 images usually include a significant number of low flux CR hits, the threshold for CR detection should be set low for the most effective CR cleaning. Windhorst et al. (1994) suggest for the original WF/PC an optimal clipping level of about 2 to $2.5 \sigma_{\text{Poisson}}$. At such a low level, many peaks of the noise will be flagged as CR hits. It is therefore important that both points deviant in positive and negative direction are rejected in order to avoid biasing of the background level.

A total of 100 iterations were used, and the CR removal on a 2σ level was started after 20 iterations. The result is shown in panel S of Fig. 1. It can be seen that this approach retains all the resolution gain of the sub-pixel shifts, but removes CR hits as effectively as the median of the unshifted images. Note in particular that even at the position of the CR hits, the co-added image approximates the “true” image much closer than both the single observations and the Richardson-Lucy restoration.

4. CONCLUSIONS

CR hits on undersampled images such as those taken with WFPC2 can be found and removed through simultaneous restoration of shifted images. The procedure is very robust and does not depend very much on parameters used. The net effect of a CR hit when dealt with in that manner is locally increased noise and lower resolution, because the resolution enhancement and noise reduction gained from the additional shifted image is locally lost. While such a local loss of information is unavoidable, no interpolation is used. Therefore, the degree of local loss of resolution is small. The method is easy to build into existing restoration codes. The availability of a method which simultaneously addresses CR hits and the undersampling of the PSF by the WFPC2 camera suggests that sub-pixel shifts between exposures is a viable strategy to recover resolution of undersampling cameras. For WFPC2, the programs most likely to profit from such a strategy are images of large bright objects, which cannot be easily placed on the PC chip and for which a high S/N can be achieved. The above simulation used a wide bandpass filter roughly in the center of the WFPC2 wavelength coverage. The undersampling is already significant at this wavelength, and the sub-pixel shifts can recover fine structure which otherwise would be lost. The only caveat is that because of the position dependence of the PSF within each CCD chip in WFPC2, such a resolution-enhancement technique can be applied only to a part of an image at a time.

I thank Bob Fosbury for suggesting this project, Richard Hook for his co-adding code and advice, and Leon Lucy for valuable discussions and reading a draft of this paper. The

software discussed in this paper, which can be compiled under both IRAF and MIDAS, is available via anonymous ftp from ecf.hq.eso.org.

REFERENCES

- Freudling, W. 1993, ST-ECF Newslett., 20, 8
 Freudling, W. 1994a, in *The Restoration of HST Images and Spectra II*, ed. R. J. Hanish and R. L. White, 264
 Freudling, W. 1994b, Internal ECF Memorandum
 Freudling, W. 1994c, ST-ECF Newslett., 21, 6
 Hook, R., and Lucy, L. B. 1992, ST-ECF Newslett., 17, 10
 Hook, R., and Lucy, L. B. 1993, ST-ECF Newslett., 19, 6
 King, I. R., et al. 1991, AJ, 102, 1553
 Lucy, L. B. 1974, AJ, 79, 745
 Lucy, L. B. 1991, ST-ECF Newslett., 16, 6
 Lucy, L. B., and Baade, D. 1989, in *Proc. 1st ESO/ST-ECF Data Analysis Workshop*, Garching, April 1989, ed. P. Grosbøl, R. H. Warmels, and F. Murtagh, p. 219
 Press, W. H., Flannery, B. P., Teukolsky, S. A., and Vetterling, W. T. 1986, *Numerical Recipes* (Cambridge, Cambridge University Press).
 Richardson, W. H. 1972, J. Opt. Soc. Am., 62, 55
 Snyder, D. L., Hammoud, A. M., and White, R. L. 1993, J. Opt. Soc. Am. A, 10, 1014
 White, R. L. 1993, in *Restoration: Newsletter of STScI's Image Restoration Project*, ed. R. J. Hanisch (Baltimore, STScI), p. 11
 Windhorst, R. G., Franklin, B. E., and Neuschaefer, L. W. 1994, PASP, 106, 798